PHYSICAL REVIEW B VOLUME 5, NUMBER 8 15 APRIL 1972

Nuclear Spin-Lattice Relaxation in the $La_{1-c}Gd_cAl_2$ Intermetallic Compounds*

M. R. McHenry[†,‡] and B. G. Silbernagel[‡]
Department of Physics, University of California, Santa Barbara, California 93106

and

J. H. Wernick
Bell Laboratories, Murray Hill, New Jersey 07974

(Received 12 October 1971)

The contribution of Gd impurities to the spin-lattice relaxation of La^{139} and Al^{27} nuclei in the compound $La_{1-c}Gd_cAl_2$ is studied for values of c from 0.0013 to 0.10, applied magnetic fields between 3.6 and 24.4 kOe, and temperatures from 1.2 to 300 K. The impurity component of the magnetization recovery for Al^{27} is characterized by an $\exp[-(t/\tau_1)^{1/2}]$ time dependence, indicating diffusionless relaxation of the nuclei to the impurity. The recovery rate $1/\tau_1$ has a temperature and magnetic field dependence described by the derivative of the Brillouin function, and is found to be proportional to the impurity concentration. Longitudinal dipolar fluctuations of the Gd moments are the principal source of the impurity relaxation, and these fluctuations result from a spin-spin interaction between impurities. An analysis in the free-electron approximation indicates that a Ruderman-Kittel-Kasuya-Yosida coupling is the source of this interaction and yields a value of $J_{sf} \simeq 0.09$ eV for the strength of the conduction-electron–rare-earth coupling constant. A comparison is made with previous magnetization, susceptibility, and paramagnetic-resonance studies in the same system.

I. INTRODUCTION

We have studied the Gd impurity contribution to the spin-lattice relaxation of La^{139} and Al^{27} nuclei in the intermetallic compound $La_{1-c}Gd_cAl_2$. The special properties of the $LaAl_2$ host enable us to analyze impurity effects in a more direct way than has been possible in previous studies.[1] We are able to identify the relaxation mechanism, and use these measurements to probe the dynamics of the Gd impurity. We begin by discussing the process of interpreting impurity relaxation results and show how many of the usual difficulties are avoided in the present system.

Experimentally, we measure the recovery of the z component $M_z(t)$ of the nuclear magnetization at times t after an initial saturation of the spin system. Using such data to arrive at estimates for basic properties of the system, e.g., the strength of the impurity–conduction-electron interaction, entails an involved analysis of the data and a number of assumptions. First, the recovery of $M_z(t)$ involves both impurity relaxation and the contribution normally expected in the host material. This is not usually a problem in insulators at low temperatures, since the host relaxation is quite weak and impurity effects dominate.[2] However, the presence of the Korringa[3] mechanism in metals results in a relatively fast host relaxation rate even at liquid-helium temperatures. This complicates the separation of host and impurity effects, especially at low impurity concentrations where the host process may dominate the recovery. Even after the impurity component of the $M_z(t)$ recovery has been determined, the relation between this and the impurity relaxation process is still not unambiguous, because, in addition to being coupled to the impurities, the nuclei are coupled to each other. The resulting recovery of the impurity magnetization involves both energy transfer from the nuclei to the impurity and energy exchange among the nuclei via spin-diffusion processes.[4] A simple functional dependence occurs only in certain select cases, and determining the relationship between nuclear spin diffusion and actual relaxation by the impurity involves quantities such as the nuclear spin-diffusion constant and the cutoff radius[4,5] that are not well defined experimentally. Once the impurity relaxation rate is obtained, it is related to the basic properties of the substance by invoking some model for the relaxation process. The magnitude and fluctuation rate of the local field at the nuclear site caused by impurities in metals can be expressed in terms of the coupling strengths of the conduction electrons with the impurities and nuclei and other quantities such as the dipolar moments of both nuclei and impurities.[5] However, for the analysis to be tractable, the Ruderman-Kittel-Kasuya-Yosida (RKKY) model[6] is generally used. This simplified picture of the conduction-electron–impurity interaction and the nature of the conduction electrons represents only an initial approximation to the real situation in actual materials and must be treated with caution.[7] To summarize the situation, an interpretation of the data requires: (i) a separation of the impurity contribution to magnetization recovery from that of the host, (ii) an unambiguous relation of the impurity component of the magnetization recovery to the actual relaxation process, and (iii) a picture of the impurity relaxation in terms of the intrinsic parameters of the system.

We find that these usual difficulties are greatly minimized in the $La_{1-c}Gd_cAl_2$ system. First, the Korringa relaxation process in the $LaAl_2$ host is particularly weak for the Al^{27} nuclei, being about an order of magnitude slower than in Al metal. This simplifies the identification of the impurity contribution to the magnetization recovery discussed above. The second and most conspicuous aspect of the experimental data is the *nonexponential* recovery of the nuclear magnetization. The form observed, being proportional to $\exp[-(t/\tau_1)^{1/2}]$, is associated with diffusionless relaxation to the impurities.[8] Such a diffusionless relaxation process simplifies the analysis in two ways: The ambiguity about relaxation to the impurity and diffusion among the nuclei is removed, and the resulting expression for $1/\tau_1$ can be expressed in terms of well-defined parameters which are independent of the diffusion constant and cutoff radius. Finally, the variation of the recovery rate $1/\tau_1$ with changing magnetic field, temperature, and impurity concentration enables us to identify the impurity relaxation process and the source of impurity spin fluctuations solely on the basis of the functional dependence of the data. This means that it is not necessary to depend upon the RKKY picture for any crucial portion of the analysis. Rather, we shall use the experimental data for an examination of the model.

Section II contains a discussion of the experimental procedures and the basic observations: The recovery of the magnetization has the form $\exp[-(t/\tau_1)^{1/2}]$, the quantity $1/\tau_1$ has a magnetic field (H) and temperature (T) dependence of the form $\partial B_S(x)/\partial x$ [where $B_S(x)$ is the Brillouin function and $x = g\mu_B \times SH/k_B T$], and the value of $1/\tau_1$ is proportional to impurity concentration. In Sec. III we demonstrate that, in the absence of nuclear-spin diffusion, an appropriate average of the contributions to the nuclear relaxation from various possible impurity configurations about any given nuclear site results in the $\exp[-(t/\tau_1)^{1/2}]$ form for the magnetization recovery. The dependence of the rate on the derivative of the Brillouin function indicates that longitudinal fluctuations of the impurity dipole moment are responsible for the relaxation.[5] We then use the RKKY picture in a high-temperature approximation to calculate the fluctuation rate of the impurities, again taking a configuration average over possible impurity positions. Comparing this model calculation to the observed values of the relaxation rate, we obtain a value of the impurity–conduction-electron coupling strength of $J = 0.09$ eV.

In Sec. IV, we relate this work to other previous measurements in the system. The value of J obtained by this analysis compares well with the results of other experiments in the same system. However, the RKKY picture cannot account for the properties of magnetically dense $GdAl_2$ with the same values of J that are derived from the magnetically dilute studies. The larger J found for the dense cases suggests an enhancement of the RKKY range function for near-neighbor interactions. Finally, we do not detect any evidence of long-range magnetic order in the samples studied even at high ($c = 0.1$) concentrations. The significance of this observation will be discussed.

II. EXPERIMENTAL

A. Procedure

The samples used in these experiments were prepared by arc melting the appropriate stoichiometric amounts of 99.9%-pure La and 99.9999%-pure Al in an argon atmosphere. A series of alloys were made with the ratio c of Gd atoms to La atoms of 0.0013, 0.003, 0.01, 0.02, 0.05, and 0.10. The impurity concentration of the $c = 0.0013$ and $c = 0.003$ samples were checked by measuring the depression of the superconducting transition temperature T_c.[9] The value of T_c in our nominally undoped sample (3.10 K) indicates the presence of approximately 0.04% magnetic impurities (most likely Ce or Fe) in the host material. Buttons of the alloys were crushed and passed through a 400-mesh screen. The resulting powder was placed in a Teflon test tube and covered with Dow Corning silicon oil. X-ray diffraction studies of the initial materials and the final powders indicate only the presence of the cubic laves ($C15$) phase appropriate to those systems.[10]

The spin-lattice relaxation measurements were made using a pulsed, phase-coherent, magnetic-resonance spectrometer.[11] A dual-gating arrangement was used for the transmitter which permitted the use of different rf sources for the pulse pair used to form the spin echo and saturating train used in the T_1 measurements. The echo pulses and the reference frequency used in the receiver were produced by a Tektronix Model-191 constant-amplitude signal generator, while a swept oscillator (Kay Marka-Sweep Model π) was used for the saturating pulse train. This allowed production of rf pulses at various frequencies within the bandwidth of the transmitter (~1.5 MHz) during the saturating train.

B. Relaxation in $LaAl_2$

Since most of the impurity analysis will deal with Al^{27} relaxation studies, we discuss the details of the Al^{27} resonance measurements made in the host.

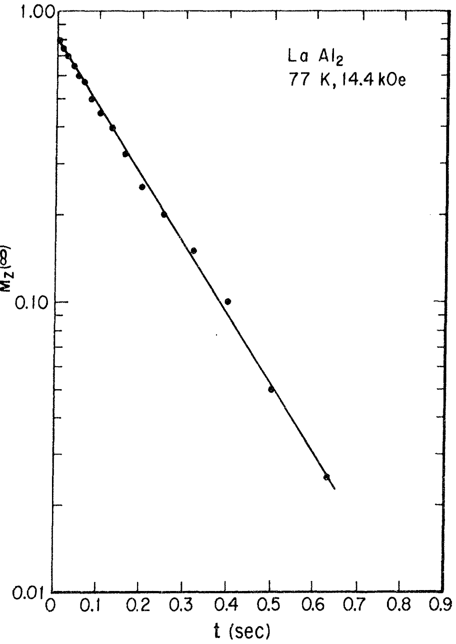

FIG. 1. Recovery of the longitudinal magnetization of the Al^{27} resonance in $LaAl_2$. A semilogarithmic plot of data taken at $T=77$ K and $H=14.4$ kOe indicates that the recovery is exponential.

In the presence of a strong quadrupolar[12] coupling ($[e^2qQ]\simeq 4.7$ MHz), it is difficult to saturate the entire powder-pattern line profile. As a result, spin-echo measurements of central portion of the line [principally of the $(\frac{1}{2}\longleftrightarrow -\frac{1}{2})$ transition] do not recover exponentially, but for the present case ($I=\frac{5}{2}$) have a magnetization recovery described as

$$1 - M_z(t)/M_z(\infty) = \alpha_1 e^{-t/T_1} + \alpha_2 e^{-6t/T_1} + \alpha_3 e^{-15t/T_1}, \tag{1}$$

where the appropriate values of the α's are determined by the initial saturation conditions.[13] For uniform saturation of the resonance line (all spins at a common spin temperature immediately after saturation) $\alpha_2=\alpha_3=0$, and the magnetization recovers exponentially.

In order to minimize the nonexponential character of the magnetization recovery, we have used a train of ~ 200 saturation pulses, of 1-2-μsec duration. The rf frequency of these saturation pulses is swept at a rate of 1 kHz over the bandwidth of the transmitter (~1.5 MHz). This procedure uniformly saturates all but the wings of the $\pm\frac{3}{2}\leftrightarrow\pm\frac{5}{2}$ transitions. A typical recovery is shown in Fig. 1 for $H=14.4$ kOe and $T=77$ K. It is well described by an exponential function with a relaxation time of 182 msec; however the saturation is only 80% complete because of the necessity of spreading the rf power over a broad linewidth. At lower temperatures this sweep saturation technique is more effective because more pulses can be applied in a time short compared to the spin-lattice relaxation time of the host, T_{1K}, which increases with decreasing temperature.

At liquid-helium temperatures, the presence of the ~0.04% of magnetic impurities in the 99.9% La used in making these samples is seen as a slightly nonexponential recovery, shown in Fig. 2, and causes a contribution to the relaxation rate. If we analyze the data as in Sec. IIC, we find values of the Korringa rate $1/T_{1K}T=0.07\pm0.005$ $(\mathrm{K\,sec})^{-1}$ and an impurity rate (at 4.2 K and an applied field of 14.4 kOe) of $0.08\pm0.04\ \mathrm{sec}^{-1}$. This is also consistent with the decrease of the superconducting transition temperature discussed in Sec. IIA.

The cubic site of the La^{139} nuclei precludes such quadrupole effects, and we find an exponential recovery for the La magnetization. The magnitude of the rate is $(1/T_{1K}T)^{139}=1.33\pm0.15$ $(\mathrm{K\,sec})^{-1}$. Impurity effects on the La^{139} resonance in this sample were not evident because $(1/T_{1K})^{139}$ is much greater than the impurity contribution even at liquid-helium temperatures. Measurements of the spin-spin relaxation times indicate values of $T_2=600$ μsec for the Al^{27} nuclei and 450 μsec for the La^{139} nuclei.

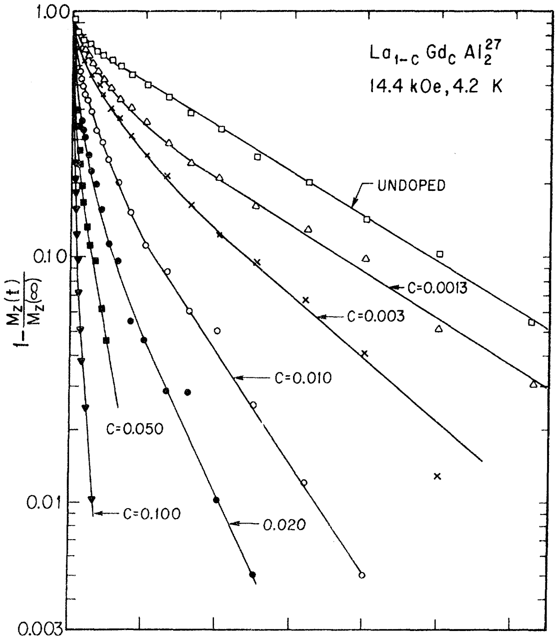

FIG. 2. Longitudinal magnetization recovery at 4.2 K and 14.4 kOe for the impurity doped samples. The recovery is decidedly nonexponential, and becomes more rapid with increasing impurity concentration.

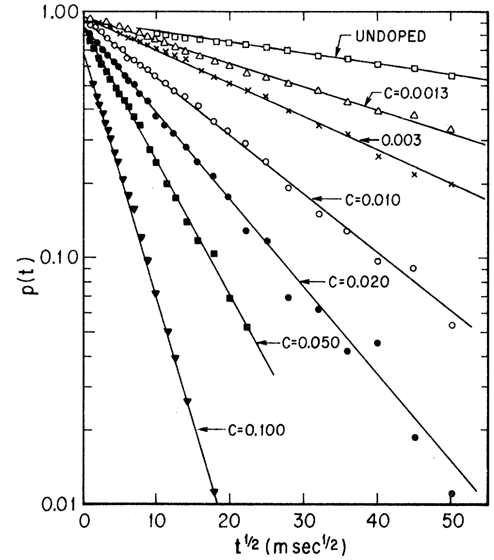

FIG. 3. The impurity component of the magnetization recovery, $p(t)$, for the situation shown in Fig. 2. The effect of host relaxation process is removed as indicated in Eq. (2). We find that $p(t)$ is an exponential function with an argument $t^{1/2}$.

C. Impurity Relaxation

The presence of Gd impurities affects the resonance properties of the Al^{27} nuclei in several ways: First, the time dependence of the magnetization recovery changes. Second, the impurity relaxation is characterized by a well-defined dependence on impurity concentration c, magnetic field H, and temperature T. Third, the resonance line is observed to broaden and the signal intensity decreases at low temperatures. We will discuss each of these results in detail.

Figure 2 shows a typical series of magnetization recoveries at 14.4 kOe and 4.2 K. The observed behavior of $M_z(t)$ results from a combination of host- and impurity-relaxation effects. We have attempted to isolate the impurity contribution by assuming that the Korringa and impurity relaxation processes are independent and have multiplied each data point by $e^{+t/T_{1K}}$ to remove the Korringa contribution.[14] The resulting impurity component $p(t)$ of the magnetization recovery, where

$$p(t)=[1-M_z(t)/M_z(\infty)]\,e^{+t/T_{1K}}, \tag{2}$$

does not recover exponentially, but rather has the form $\exp[-(t/\tau_1)^{1/2}]$. This is seen in Fig. 3, where $p(t)$ is plotted semilogarithmically as a function of $t^{1/2}$. We will analyze the parameter τ_1 which characterizes this $t^{1/2}$ decay.

We have measured τ_1 as a function of c, T, and H. Figures 4(a) and 4(b) summarize these measurements: $1/\tau_1$ is plotted as a function of the

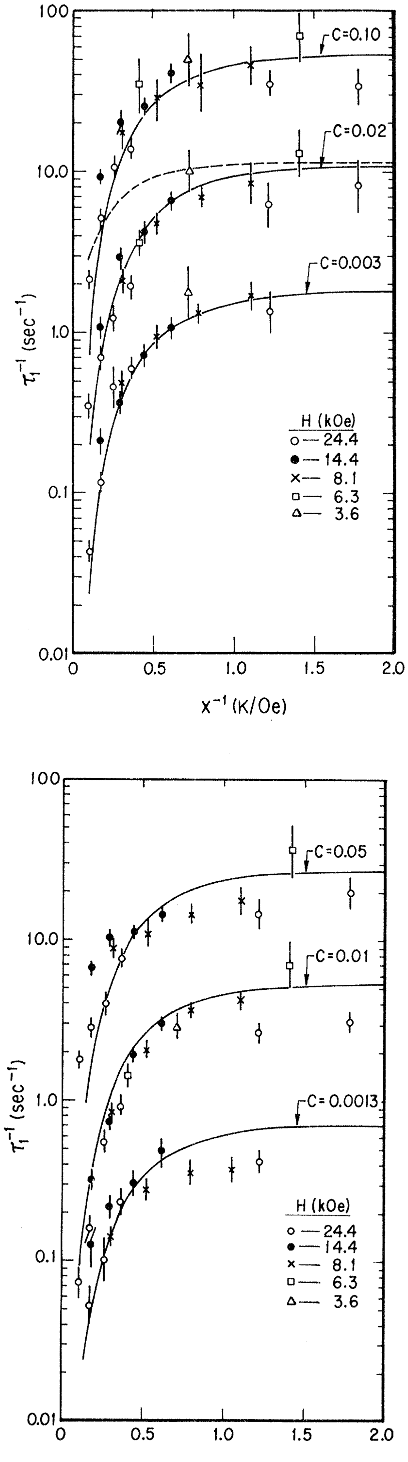

FIG. 4. Variation of the observed impurity relaxation rate with the function $x^{-1}=k_BT/g\mu_BSH$. The data taken at a wide range of field and temperature is seen to lie along a universal curve $1/\tau_1=\alpha c\;\partial B_S(x)/\partial x$ (solid curves) for any given value of the concentration. Comparison of this curve to the functions $B_S(x)/x$ (dashed curve) and $\partial B_S(x)/\partial x$ are shown for the $c=0.02$ sample.

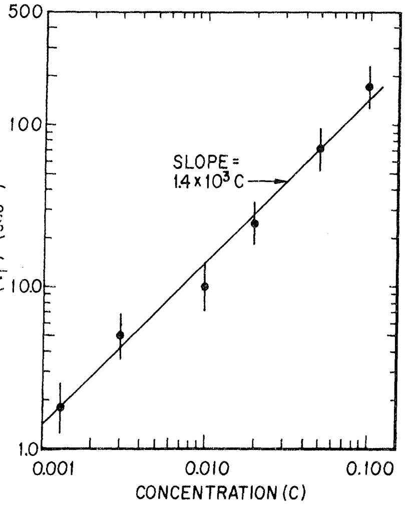

FIG. 5. Variation of the single parameter fit for the relaxation rate $1/\tau_1^0$ with concentration. This log-log plot indicates a linear dependence of $1/\tau_1^0$ with c.

parameter x^{-1}, where $x = g\mu_B SH/k_B T$. The data represent measurements for T between 1.2 and 20.4 K and H between 3.6 and 24.4 kOe. For all concentrations, we find the $1/\tau_1$ data is well described by a universal curve in this T/H plot. We compare the experiment for $c = 0.02$ in Fig. 4(a) with plots of the functions $B_S(x)/x$ and $\partial B_S(x)/\partial x$, where $B_S(x)$ is the Brillouin function of the Gd impurities [$J = S = \frac{7}{2}$ for Gd and we therefore choose to write the Brillouin function as $B_S(x)$]. We conclude that the data is best described by the *derivative* of the Brillouin function. The relation of this dependence to possible relaxation mechanisms will be discussed in Sec. III.

To analyze this data, we have obtained a best fit to each set of data points of the form

$$\frac{1}{\tau_1} = \frac{1}{\tau_1^0}\,\frac{\partial B_{7/2}(x)}{\partial x}\,. \tag{3}$$

These "best-fit values" $1/\tau_1^0$ are shown as a function of concentration in Fig. 5. This log-log plot indicates that $1/\tau_1^0$ is directly proportional to c, $1/\tau_1^0 = \mathfrak{a}c$, where $\mathfrak{a} = 1400$ sec^{-1} [27] and c is the fraction of lattice sites occupied by Gd impurities. As an indication of the self-consistency of this analysis, we show solid curves in Figs. 4(a) and 4(b) for each value of c corresponding to the expression $1/\tau_1 = \mathfrak{a}\, c[\partial B_S(x)/\partial x]$; the *single parameter* in this fit is the value $\mathfrak{a}$ given above. The fact that this data can be fit over a one-order-of-magnitude range in x and over a two-order-of-magnitude range in c with a single parameter is very striking.

Measurements of τ_1 were also made at 77 and 300 K for samples with higher impurity concentrations ($c = 0.01 - 0.10$). The much stronger Korringa relaxation at these higher temperatures complicates the process of extracting the relatively weak-impurity contribution. However, with an uncertainty of approximately 20% for the $c = 0.05$ sample we find at 77 K that

$$1/\tau_1 \simeq 1/\tau_1^0[\,(S+1)/3S]\,,$$

which is the expected high-temperature form of $\partial B_S(x)/\partial x$. Saturating the wings of the resonance line becomes progressively more difficult at lower fields. This places the lower limit ($H \sim 4$ kOe) on our τ_1 observations.

We observe considerable broadening of the resonance line at low temperatures and high fields in samples of higher impurity concentration. An example of the Al^{27} field profile for the $c = 0.05$ sample for 4.2 K and 9 MHz is compared with the undoped sample in Fig. 6. Further information about line broadening can be obtained from the variation of the amplitude of the magnetization at the center of the resonance line with changing H and T. These results are summarized for various sample concentrations in Fig. 7. At a given H and T, the variation with c of the amplitude is compared with $(1-c)^n$, where $n \simeq 28$ at 4.2 K. In terms of a "single-impurity" model, this would imply Al nuclei that are first and second neighbors of an impurity are shifted out of the range of observation by its static field. In the presence of a large quadrupole broadening and at such high concentrations, the concept of an observation barrier no longer has its previous significance. However the variation of n with H and T and an estimate of the linewidth of the $c = 0.05$ sample at 4.2 K using moment techniques[15] indicate that the increase in linewidth arises from static broadening by paramagnetic impurities.

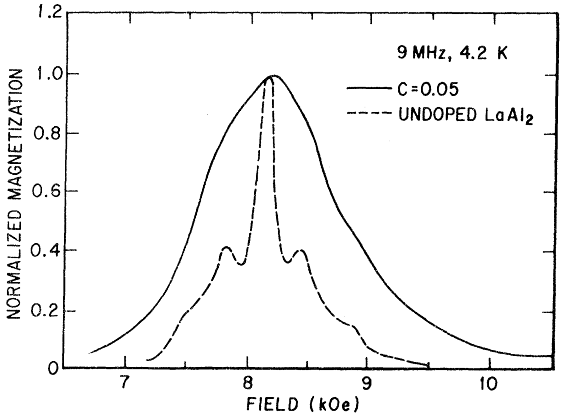

FIG. 6. Broadening of the resonance line at low temperatures. The width of the host resonance is compared with that of the $c = 0.05$ line at 4.2 K and an applied field of 8.1 kOe. The linewidth in the $c = 0.05$ sample is consistent with paramagnetic broadening.

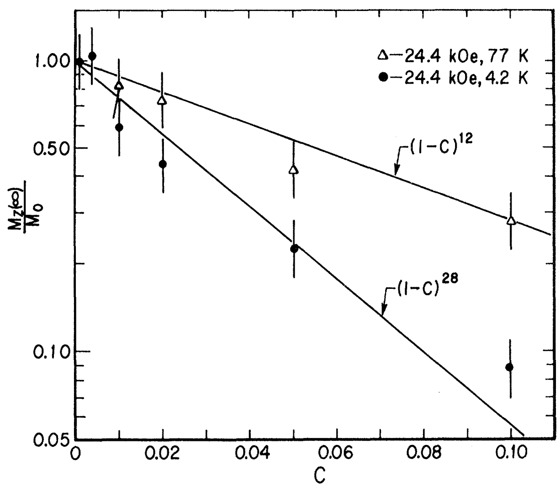

FIG. 7. Variation of wipeout with temperature as observed by monitoring the magnitude of the center of the Al^{27} resonance line (see Ref. 8). The ratio of the unsaturated value of the longitudinal magnetization $M_z(\infty)$, to the magnitude M_0 in pure $LaAl_2$, is plotted as a function of c. The data indicates an exclusion number of ~ 12 at $T=77$ K and ~ 28 at $T=4.2$ K.

Since low-field susceptibility measurements indicate the onset of magnetic order in the $c=0.05$ and $c=0.10$ samples at $T\sim5$–10 K, we would like to summarize the results of this high-field study which bear on it: First, there is no obvious shift of the center of the resonance line at low temperatures, and its width is consistent with the estimates associated with polarization of paramagnetic spins. Second, to within an accuracy of ~20% the integrated intensity of the line profile for the $c=0.05$ sample at 9 MHz and 4.2 K (see Fig. 6) is the same as that for the undoped sample. Finally, there is no evidence in the relaxation data of the critical fluctuations usually associated with the onset of such order. Thus, even at $c=0.10$, the sample behaves like a paramagnet for the range of H and T studied. Measurements at the wings of the profile lead to approximately the same value of τ_1 as seen at the center. We will relate these results to the problem of magnetic order in Sec. IV.

The resonance results for impurity relaxation of La^{139} are much less extensive. As mentioned in Sec. II B, the Korringa relaxation in the host is twenty times more rapid for the La^{139} nuclei than it is for the Al^{27} nuclei, and the impurity relaxation rates are comparable, which makes isolation of $p(t)$ much more difficult, particularly in low-concentration samples. Strong impurity broadening of the La^{139} resonance limited measurements to samples with $c\leq0.02$ at low temperatures. The value of the spin-spin relaxation time is observed to lengthen dramatically at low temperatures (from $T_2\sim400$ μsec at $T=77$ K and $H=15$ kOe to $T_2\sim1.7$ msec at $T=4.2$ K and $H=15$ kOe for the $c=0.02$ sample). Subject to the qualifications mentioned above $p(t)$ was fit to an $\exp[-(t/\tau_1)^{1/2}]$ time dependence. The resulting values of τ_1 appear to exhibit the $\partial B_S(x)/\partial x$ behavior, with a strength, expressed in terms of Eq. (3) and the discussion following, of $\mathcal{A}^{139}=1370\ \mathrm{sec}^{-1}$.

III. INTERPRETATION

To analyze this data, we will follow the procedure outlined in Sec. I: relating $M_z(t)$ to the relaxation process, using the field and temperature dependence of τ_1 to identify the relaxation mechanism, and finally using an RKKY model to calculate the fluctuation rate of the magnetic impurities. At each stage we will compare the predictions of the model with the experimental data of Sec. II.

A. Magnetization Recovery

We will assume that the Korringa process affects all the nuclei in a uniform way, which is independent of the impurity relaxation mechanism. We then confine our attention to the impurity component $p(t)$ of the magnetization recovery, as defined in Eq. (2). The observed behavior of $p(t)$ is related to three factors characteristic of the system: relaxation, nuclear spin diffusion, and exclusion. The first is the relaxation itself, arising from fluctuations of the impurity field at the nuclear site. The relaxation rate $1/T_1(r_{ij})$ for a nucleus at position $\vec{r}_i$ resulting from an impurity at position $\vec{r}_j$ ($r_{ij}=|\vec{r}_i-\vec{r}_j|$) can be estimated from perturbation theory if the magnitude of the impurity field and the impurity fluctuation rate can be determined.[16] The nuclei are not uniformly affected since this field falls off rapidly ($\propto 1/r_{ij}^3$). These rate calculations will be discussed in Sec. III B, but for the sake of the present arguments we assume $1/T_1(r_{ij})=\mathcal{C}/r_{ij}^6$ for its form. The basic problem is to be able to arrive at the behavior of the macroscopic quantity $p(t)$, representing an ensemble average of nuclei in various different environments using this microscopic information about the relaxation rate.

The two other factors mentioned above generally complicate this problem. In many solids, the spin-spin interaction between the nuclei is strong and energy in the nuclear spin system can diffuse from one position in the sample to another by mutual nuclear spin flips.[17] Further, nuclei sufficiently close to an impurity may be shifted out of the range of observation by the impurity's static field. Nuclei lying within this cutoff radius r_0 are not retained in performing the ensemble average leading to $p(t)$.

Thus the recovery to equilibrium for a nucleus at the site $\vec{r}_i$, $p(\vec{r}_i,t)$, should be described by[4]

$$\frac{\partial p(\vec{r}_i,t)}{\partial t}=D[\nabla^2 p(r,t)]_{r=\vec{r}_i}-p(\vec{r}_i,t)\sum_j\frac{1}{T_1(r_{ij})}, \qquad (4)$$

where both the effects of spin diffusion and relaxation to the impurity are explicitly considered. The observed $p(t)$ should be the spatial average of $p(\vec{r}_i,t)$, which we will denote by double brackets, i.e., $p(t)=\langle\langle p(\vec{r}_i,t)\rangle\rangle$. Nuclei lying within r_0 of any impurity are excluded from the average. The form taken by $p(t)$ will be quite complex in general[2,4] and will depend on the relative values of $D, \mathcal{C}$, r_0, and the mean impurity spacing $R=(3/4\,\pi N_0 c)^{1/3}$, where N_0 is the density of rare-earth sites. However in the case of $LaAl_2$, the very weak spin-spin interaction (resulting in a spin-spin relaxation time $T_2\sim 600$ μsec as opposed to $T_2\sim 20$ μsec in Al metal) and the close proximity of all nuclei to impurities resulting from relatively high impurity concentrations should tend to minimize diffusion effects. We will therefore examine the consequences of choosing $D=0$ in Eq. (4). We present a numerical argument justifying this assumption later.

If $D\sim 0$, the solution of Eq. (4) becomes[8]

$$p(r_i,t)=\exp\{-t\textstyle\sum_j[1/T_1(r_{ij})]\}, \tag{5}$$

where j is summed over impurity sites. At any given point $\vec{r}_i$, the recovery is exponential. However the configuration of impurities seen by the nuclei will vary from site to site, leading to a distribution in relaxation rates. The resulting configuration average leading to $p(t)$ is not expected to be exponential. Because of the unique form of Eq. (5), $p(t)$ can be expressed as the product of contributions from each of the impurity sites as indicated in Eq. (A2) of Appendix A. We have used this product representation to evaluate $p(t)$ numerically for various forms of $1/T_1(r_{ij})$. These calculations were performed on an IBM-360 model-75 computer, the product being taken over 4093 adjacent rare-earth lattice sites. However, for low concentrations ($c\ll 1$), the configuration average can be evaluated in a continuum model, resulting in an expression for $p(t)$ [Eq. (A5)] with an asymptotic long-time dependence of the form $\exp[-(t/\tau_1)^{1/2}]$, where

$$1/\tau_1=(\tfrac{4}{3}\pi^{3/2}N_0c)^2\,\mathcal{C}\ . \tag{6}$$

Note that Eq. (6) does not involve the exclusion radius. This removes much of the ambiguity from our interpretation of magnitudes of τ_1. The effect of a finite exclusion radius r_0 is to cause deviations from this behavior at short times. In fact, we show in Appendix A that for $\mathcal{C}t/r_0^6\ll 1$, $p(t)$ is exponential. The over-all effect is illustrated in Fig. 8 where calculations are made for a hypothetical sample with $c=0.02$ and a value of $\mathcal{C}=1.2\times10^{-42}$ cm^{6}sec^{-1}, comparable to that deduced from our relaxation measurements. A semilogarithmic plot of $p(t)$ vs $t^{1/2}$ for various values of r_0 illustrates the asymptotic $t^{1/2}$ long-time behavior and the bending over of the curve at short t. The solid curves represent the analytic form for $p(t)$, Eq. (A5), derived in the low-concentration limit, while the dots are numerical calculations of the product form, Eq. (A2). The agreement between the numerical calculation, which involves no assumptions about concentration, and the low-density continuum model is very good and remains so even for $c=0.1$.

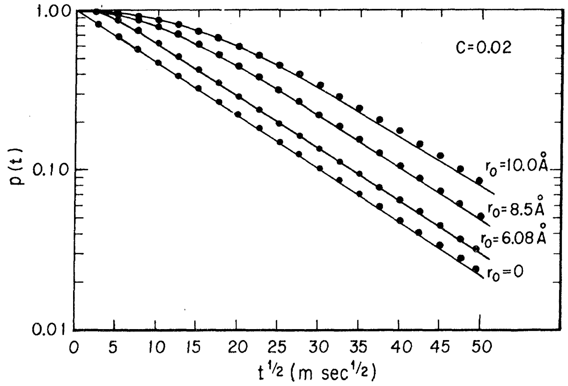

FIG. 8. Impurity component of the magnetization recovery in the diffusionless limit. We plot the $\log_{10}$ of $p(t)$ as a function $t^{1/2}$ for the $c=0.02$ sample, assuming $\mathcal{C}=1.2\times10^{-42}$ cm^6 sec^{-1}. The units of $t^{1/2}$ are msec$^{1/2}$ and r_0 indicates the exclusion radius for each calculation. The solid lines represent the results of an analytic solution in the low-concentration limit, while the dots are the results of the general numerical analysis.

Before completing this discussion we would like to analyze two of the assertions made in a quantitative way: the contention that the process is diffusionless and the assertion that for these measurements $\mathcal{C}t/r_0^6\gg 1$. These problems have been considered in some detail[2,18] in the single-impurity limit ($c\ll 1$). However, in the present case, with relatively high concentrations of impurities, severe quadrupolar broadening of the Al^{27} nuclear resonance even in the host material, and the presence of an oscillating impurity field from RKKY polarization of the conduction electrons, the usual conditions for a diffusionless process based on the single-impurity model can only be regarded as suggestive. We will make these numerical estimates for the $c=0.0013$ sample, which most nearly satisfies this single-impurity criterion. In this model the condition[2] for weak diffusion is $(\mathcal{C}/D)^{1/4}\gg R$. This will clearly be most severely tested at low concentrations when R becomes large. From the results of Sec. III B, we find $\mathcal{C}\simeq 4.7\times10^{-44}/c$ cm^{6}sec^{-1}. For the $c=0.0013$ sample, the weak diffusion condition would be expected in the case $D\ll\mathcal{C}/R^4\simeq 10^{-14}$ cm^{2}sec^{-1}. It is difficult to evaluate D accurately, but we can obtain an order-of-magnitude estimate[17] from the relation $D\sim a_0^2/50T_2$, where $a_0\simeq 2.9$ Å and $T_2\simeq 0.6$ msec. The value obtained, $D\sim 3\times10^{-14}$ cm^{2}sec, is somewhat larger than the upper limit required for a diffusionless case. However, other factors, most notably the RKKY oscillations of the local field and the quadrupolar splitting of the nuclei,[25] will tend to reduce the effect of diffusion even below the prediction given above. It will be an even better approximation at higher concentrations. Similarly, we would like to identify the region in which the bending over in the $p(t)$ curve occurs: $\mathfrak{C}t/r_0^6 \sim 1$. Taking $r_0 = 6$ Å corresponding to the exclusion observations of Sec. II C, and the value of $\mathfrak{C}$ appropriate to the $c = 0.0013$ sample above, we find $t \sim r_0^6/\mathfrak{C} = 1$ msec. Thus our observations should be well into the asymptotic long-time region for $t \gtrsim 10$ msec. As indicated above, $\mathfrak{C}$ is proportional to $1/c$, so this criterion becomes more difficult to satisfy as the concentration increases. If the single-impurity model were correct in the $c = 0.1$ case, $p(t)$ would not reach its asymptotic form until $t \sim 100$ msec. This behavior is not observed experimentally (see, e.g., Fig. 3), indicating a breakdown of the single-impurity picture at high concentrations.

B. Relaxation Mechanisms

Having established the significance of the recovery rate $1/\tau_1$, we discuss the various possible impurity-relaxation mechanisms and their relative strengths in $\mathrm{La}_{1-c}\mathrm{Gd}_c\mathrm{Al}_2$. As mentioned in Sec. I, such a study can proceed qualitatively by an analysis of the functional dependence of $1/\tau_1$ as H, T, and c are varied. Alternatively the order of magnitude of the rate from various processes can be estimated within the context of the comparatively simple RKKY analysis. We shall use an RKKY model wherever necessary in estimates of the relaxation rate and the relevant parameters needed for such estimates are included in Table I. We have chosen our notation to be consistent with Ref. 5, except that $N(E_F)$ replaces the quantity $N(0)/N$ which appears in that paper. We assume a free-electron picture for the Fermi-surface electrons, with each atom contributing three electrons to the band.

TABLE I. Characteristic parameters for $\mathrm{La}_{1-c}\mathrm{Gd}_c\mathrm{Al}_2$.

Lattice constant[a]	a_0	8.145 Å
Molecular density[a]	N_0	1.48×10^{22} cm^{-3}
Fermi momentum[b]	k_F	1.58 Å^{-1}
Fermi energy[b]	E_F	9.5 eV
Density of states at the Fermi surface[b]	$N(E_F)$	0.47 states eV^{-1} atom^{-1}
Gd electronic gyromagnetic factor[c]	γ_m	1.76×10^{7} sec^{-1} Oe^{-1}
Al nuclear gyromagnetic factor[c]	γ_n	6.97×10^{3} sec^{-1} Oe^{-1}
Gd spin	S	$\frac{7}{2}$
Al hyperfine constant[d]	A	0.9×10^{-6} eV

[a] Reference 9.

[b] From the free-electron model assuming $z = 3$ electrons per atom.

[c] Varian NMR table.

[d] Calculated from LaAl_2 relaxation rate.

TABLE II. Impurity relaxation mechanisms in metals.

Longitudinal dipolar (LD)

$$\left\langle \frac{1}{T_1(r,\theta)} \right\rangle_{\mathrm{LD}} \equiv \frac{\mathfrak{C}_{\mathrm{LD}}}{r^6} = \frac{1}{r^6}\left(9(\gamma_m\gamma_n\hbar)^2 S^2 \frac{\partial B_S(x)}{\partial x} \frac{\tau_{m1}}{1+(\omega_n\tau_{m1})^2}\right)\sin^2\theta\cos^2\theta$$

Transverse dipolar (TD)

$$\left\langle \frac{1}{T_1(r,\theta)} \right\rangle_{\mathrm{TD}} \equiv \frac{\mathfrak{C}_{\mathrm{TD}}}{r} = \frac{1}{r^6}\left(\frac{1}{2}(\gamma_m\gamma_n\hbar)^2 S^2 \frac{B_S(x)}{x} \frac{\tau_{m2}}{1+(\omega_m\tau_{m2})^2}\right) \times [(1-3\cos^2\theta)^2 + 9\sin^4\theta]$$

Benoit–de Gennes–Silhouette (BGS)

$$\left\langle \frac{1}{T_1(r)} \right\rangle_{\mathrm{BGS}} \equiv \frac{\mathfrak{C}_{\mathrm{BGS}}}{r^6} = \frac{1}{r^6}\left[\left(\frac{\pi AJN^2(E_F)E_F}{2\hbar k_F^3}\right)^2 S^2 \frac{B_S(x)}{x} \frac{\tau_{m2}}{1+(\omega_m\tau_{m2})^2}\right]$$

Giovannini–Heeger (GH)

$$\left\langle \frac{1}{T_1(r)} \right\rangle_{\mathrm{GH}} \equiv \frac{\mathfrak{C}_{\mathrm{GH}}}{r^5}\left[\left(\frac{\pi AJN^2(E_F)E_F}{2\hbar k_F^3}\right)^2 S^2 \frac{B_S(x)}{x} \frac{\hbar k_F}{E_F}\right]$$

Impurity relaxation in metals has been the subject of a recent review,[5] in which the various relaxation mechanisms are discussed. In addition to relaxation from longitudinal (LD) and transverse (TD) fluctuations of the impurity's dipolar field which are also common to magnetic insulators,[2] an impurity can relax the nuclei via its polarization of the conduction electrons, originally suggested by Benoit, de Gennes, and Silhouette (BGS),[19] and via virtual scattering processes, suggested by Giovannini and Heeger (GH).[20] In the context of the RKKY model and assuming an exponential decay of the longitudinal and transverse impurity-spin correlations with decay rates $1/\tau_{m1}$ and $1/\tau_{m2}$, respectively, it is possible to obtain expressions for the quantity $1/T_1(r_{ij})$ discussed in Sec. III A. We present the results for the four mechanisms discussed above in Table II. In order to be able to present a simple discussion of results, we have averaged over the trigonometric parts of the range function which occur in the expressions for $[1/T_1(r)]_{\mathrm{BGS}}$ and $[1/T_1(r)]_{\mathrm{GH}}$. The resulting simplification of the r dependence enables us to use the analytic low-concentration expression [Eq. (A4)] in our analysis. However, we have also performed calculations in which the full trigonometric forms[5] are preserved, using the product expression [Eq. (A2)] and evaluating the result by computer. The differences be-

TABLE III. Estimates of relaxation rates for several mechanisms: $c=0.01$, $T=4.2$ K, $H=14.4$ kOe, $J=0.1$ eV, $\tau_m=5.8\times10^{-11}$ sec.

	LD	TD	BGS	GH[a]	Expt.
$(1/\tau_1)$ sec^{-1}	3.4	0.10	0.02	5×10^{-5}	3.0

[a] For definition of τ_1 for GH, see Appendix A.

tween the values of τ_1 obtained in these two ways are very small.

From Eq. (6), it is clear that all field and temperature dependence of τ_1 is associated with $\mathfrak{C}$. In addition to factors like $B_S(x)$ and ω_m which obviously vary with H and T, there is also the possibility that τ_{m1} and τ_{m2} might have such a dependence. However, on the basis of recent EPR studies of Gd in $LaAl_2$,[21] which we will discuss in Sec. IV, it appears that RKKY exchange narrowing of the dipolar fields is the major contribution to the Gd linewidth at liquid-helium temperatures and that the resulting correlation times $\tau_{m1}\sim\tau_{m2}$ are independent of field and temperature and have a magnitude $1/\tau_m\simeq 2.9\times10^{12}c$. From this estimate of τ_m we observe that $(\omega_n\tau_m)^2\ll1$ for the fields and concentrations that we have studied. Thus, the only field and temperature dependence of the LD mechanism is $\partial B_S(x)/\partial x$, in good agreement with the observed behavior of $1/\tau_1$ shown in Figs. 4(a) and 4(b). Therefore, on the basis of the EPR observations which provide necessary information about the dynamics of the impurities, we are able to identify the relaxation as resulting from LD process solely on the basis of the functional dependence of τ_1.

It is also possible to obtain a quantitative estimate of the contributions to $1/\tau_1$ from the various mechanisms. The extreme simplicity of the model must be remembered in attaching significance to such calculations, but the order of magnitude of the results are instructive. The magnitudes of these mechanisms are compared with the observed value of τ_1 in Table III for a typical set of experimental conditions. In agreement with our functional analysis, it is evident that the LD mechanism is the dominant process and the magnitude of $1/\tau_1$ is in good agreement with experiment. We also note that $(\omega_m\tau_m)^2\simeq75$ for $c=0.01$ and $H=10$ kOe, so the factor $1+(\omega_m\tau_m)^2$ in the denominator of the TD and BGS mechanisms has greatly reduced their strength in large magnetic fields and for low impurity concentrations.

An especially significant consequence of the dominance of the LD process, is that the RKKY mechanism is only involved in determining the impurity dynamics and plays no role in the magnitude of the impurity field seen by the nucleus. This enables us to perform a particularly direct analysis of the RKKY model in determining the rate $1/\tau_m$. As discussed above, EPR results yield a value $1/\tau_m=2.9\times10^{12}c$ sec^{-1}. We can obtain a value for τ_m by comparing the results of our experiments [Eq. (3)] with the prediction for $1/\tau_1$ from the LD process. Using the expression for $\mathfrak{C}_{\text{LD}}$ from Table II and Eq. (A4), we find

$$\left(\frac{1}{\tau_1}\right)_{\text{LD}}=\frac{16\pi^3}{9}\,(\gamma_m\gamma_n\hbar N_0\,cS)^2\,\frac{\partial B_S(x)}{\partial x}\,\tau_m\,. \tag{7}$$

Using the experimental value of $1/\tau_1^0$ obtained in Sec. II C ($1400c$ sec^{-1}), the resulting value for the correlation rate is found to be $1/\tau_m=1.75\times10^{12}c$ sec^{-1}, in reasonable agreement with the EPR results. These results differ slightly from those reported earlier. This is because we previously averaged the angular dependence of $1/T_1(r)$ before performing the integral in Eq. (A4). We believe that the present procedure is more appropriate, and results in a change in the numerical factor of Eq. (7) from $\frac{32}{15}$ to $\frac{16}{9}$. This results in an increase of 20% in the estimate of τ_m.

C. Spin Dynamics

Having obtained two experimentally determined values of $1/\tau_m$, we would like to test whether the assumption of an exponential decay of the autocorrelation function and the magnitude of the rate can be justified in the context of the RKKY picture.

In Appendix B, we discuss a simple model for the spin dynamics of a randomly distributed collection of magnetic impurities coupled by an RKKY Hamiltonian, Eq. (B1). In the high-temperature limit, the autocorrelation function $\langle S_j^z(t)S_j^z(0)\rangle$ can be studied by performing a short-time expansion. For the purposes of the present simple estimate, we will neglect the effect of pair correlations, and assume that the decay of $\langle S_j^z(t)S_j^z(0)\rangle$ can be described by a Gaussian time dependence. Recent detailed calculations[22] in magnetic insulators indicate that this is an oversimplification of the problem, but the numerical error associated with such a model should not exceed a factor of 2.

To determine the dynamics for an ensemble of such spins, we must perform a configuration average over the possible arrangements of magnetic impurities about any given impurity site. In the absence of pair correlations between the impurities, the spatial average $\langle\!\langle\,\langle S_j^z(t)\,S_j^z(0)\rangle\,\rangle\!\rangle$ has an exponential time dependence in the limit of small impurity concentrations. The characteristic decay time is found from Eq. (B9):

$$1/\tau_m=\tfrac{1}{9}\left[\tfrac{1}{6}\,\pi S(S+1)\right]^{1/2}N(E_F)J^2c/\hbar\,, \tag{8}$$

where we have assumed $N(E_F)=3z/2E_F$, $k_F^3=3\pi^2\times(3N_0z)$, and $z=3$ conduction electrons per atom. This transition from Gaussian to exponential behavior at small c is the exact analog of the change

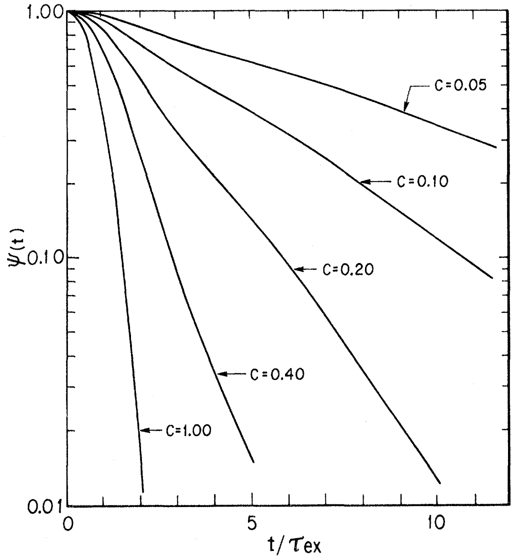

FIG. 9. Decay of the impurity autocorrelation function $\psi(t)$ for varying concentrations of impurities plotted as a function of t/τ_{ex} [τ_{ex} is defined in Eq. (B7)]. The form of the decay of $\psi(t)$ is assumed to be Gaussian at high concentration, but becomes more exponential with progressive dilution.

of the nuclear magnetization recovery from exponential to $\exp[-(t/\tau_1)^{1/2}]$ in the small-c limit. It is for this reason that we chose to characterize the decay of the correlation function by an exponential in Sec. III B.

This observation about the spin dynamics was initially made by Kittel and Abrahams,[23] who used moment methods to demonstrate the change of the EPR line profile from Gaussian to Lorentzian at large dilution. They estimated that the transition region should be around $c \sim 0.01$. Within the limits of the present model, we can calculate $\langle\langle \langle S_j^z(t) \times S_j^z(0) \rangle \rangle\rangle$ for *arbitrary c*, using the product notation, Eq. (B8), and numerical methods. The results of such a calculation are presented in Fig. 9, where the quantity $\psi(t) \propto \langle\langle \langle S_j^z(t) S_j^z(0) \rangle \rangle\rangle$ is plotted semilogarithmically as a function of t. As expected from the model the decay of the correlation function is Gaussian for $c = 1.0$, and becomes progressively more exponential as the concentration diminishes. We can establish a direct connection with the moment approach by using the reasoning of Anderson and Weiss.[24] We say that the width of the EPR profile in this case should be $\Delta H \propto M_2 \langle \tau_e \rangle$, where

$$\langle \tau_e \rangle = \int_0^\infty \langle\langle \langle S_j^z(t) S_j^z(0) \rangle \rangle\rangle \, dt \, .$$

For a Gaussian decay, we expect $\langle \tau_e \rangle \propto c^{-1/2}$, while for exponential decay, $\langle \tau_e \rangle \propto c^{-1}$. In Fig. 10 we present a plot of $\langle \tau_e \rangle$ determined from the calculations discussed above. Since the data is nearly proportional to c^{-1} for $c \leq 0.10$, we feel justified in using the exponential form of the correlation function in describing all of our results.

Using our model for the dynamics, we can arrive at a prediction for the value of J on the basis of Eq. (8) and our observed value of $1/\tau_m = 1.75 \times 10^{12} c$ sec^{-1}. In the free-electron picture, we arrive at a magnitude of the sf coupling of $|J| = 0.09$ eV, which is in extremely good agreement with previous observations. We will discuss the significance of this result in Sec. IV.

D. La^{139} Results

Since the La^{139} data are not nearly as precise as those of the Al^{27}, we do not wish to analyze it in great detail, but several basic factors are worth consideration. Both the Knight shift[12] and the relaxation rates indicate that the La^{139} nuclei are strongly coupled to the conduction electrons and are sensitive to their partial non-s character. Although nominally situated at a site of cubic symmetry, its quadrupole moment makes the La^{139} nucleus sensitive to any distortions of the lattice which occur. The presence of strains in the material could explain the large value of T_2($\sim$450 μsec) observed in the host.[25] The large increase in T_2 observed at low temperatures probably results from further decoupling of the spin-spin interaction caused by RKKY polarization of the conduction electrons by the magnetic impurity. These effects can combine to produce a diffusionless recovery

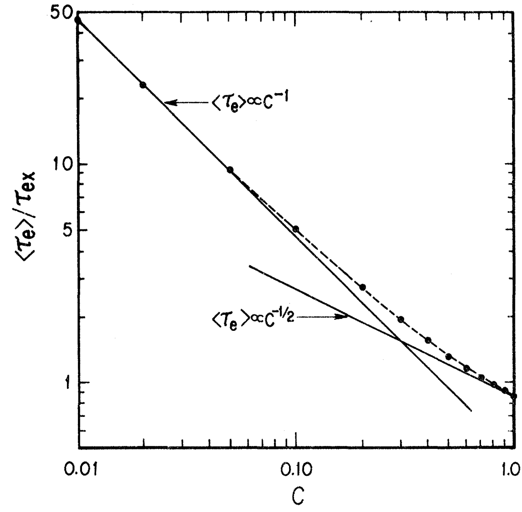

FIG. 10. Investigation of the change in character of the decay of $\psi(t)$ at low concentration. The symbol $\langle \tau_e \rangle$ represents the integral of $\psi(t)$ for all positive values of time. The reduced quantity $\langle \tau_e \rangle / \tau_{ex}$ is plotted logarithmically as a function of concentration. We find $\langle \tau_e \rangle \propto c^{-1}$ for $c \leq 0.1$, indicating exponential decay of the correlation function for all values of interest in these experiments.

in the La^{139} case as well.

An interesting aspect of the La^{139} data is that the relaxation rate $(1/\tau_1^0)^{139}$ is almost identical to that observed for Al^{27}. Since our analysis of the Al^{27} results enable us to obtain a complete picture of the impurity dynamics, we can compare predictions for $1/\tau_1^0$ for the two nuclear species to obtain a value for the impurity field at the La site. The functional dependence of $1/\tau_1$ indicates that longitudinal fluctuations of the impurity field are the dominant relaxation mechanism. However, if only the LD process were operative in both cases, one would expect from Eqs. (3) and (7) that the ratio of the relaxation strengths would be

$$(1/\tau_1^0)^{27}/(1/\tau_1^0)^{139} = (\gamma^{27}/\gamma^{139})^2 = 3.4 . \tag{9}$$

The fact that this ratio is observed experimentally to be nearly equal to one, indicates that an additional contribution to the impurity field, presumably from a pseudodipolar interaction,[26] must exist for the La nuclei. This is consistent with the other observations.

IV. DISCUSSION

In this section, we relate these present results to previous studies in the $La_{1-c}Gd_cAl_2$. We discuss the values of J obtained in the interpretation of various experiments, contrast the nature and strength of the interaction at high and low Gd concentration, and discuss possible magnetic order at low temperatures in the dilute systems.

Using the RKKY model, values of J can be readily obtained from EPR studies of Gd impurities in $LaAl_2$, the depression of the superconducting transition temperature T_c of $LaAl_2$ by Gd impurities, and impurity broadening of the La^{139} linewidth. The electron-spin resonance studies are especially interesting, since three parameters are related to J: the g shift (Δg), the Korringa contribution to the linewidth (ΔH_K), and the temperature-independent component of the linewidth (ΔH_e). In measurements on a sample with $c = 0.0045$, values of $\Delta g = +0.027$, $\Delta H_K = 22.5T$ Oe, and $\Delta H_e = 51$ Oe were reported.[21] In this free-electron picture,[7] $\Delta g = JN(E_F)$, which implies $J = +0.057$ eV. If the EPR is not bottlenecked,[27]

$$\Delta H_K = \pi N^2(E_F) J^2 k_B T/\gamma_m \hbar \quad ,$$

with a resulting prediction of $|J| = 0.066$ eV. Finally, if we attribute the temperature-independent component ΔH_e to exchange narrowing of the Gd-Gd dipolar interaction by an RKKY coupling between the spins, we expect[28] $\gamma_m \Delta H_e = M_2 \langle \tau_e \rangle$, where $\langle \tau_e \rangle$ is evaluated as in Appendix B, and M_2 is the second moment of the dipolar interaction among impurities.[23] The resulting value of the correlation rate obtained from this analysis is $1/\langle \tau_e \rangle \equiv 1/\tau_m = 2.9 \times 10^{12} c$ sec^{-1}, and using Eq. (8), we find $|J| = 0.11$ eV. Also note that the Korringa-relaxation rate, $1/\tau_K = \gamma_m \Delta H_K \simeq 4 \times 10^8 T$ sec^{-1}, is much smaller than the exchange-correlation rate at liquid-helium temperatures. It is for this reason that we neglected Korringa effects in calculating the decay rate of the impurity correlations.

Measurements of the depression of T_c by Gd in $LaAl_2$ give the value $(dT_c/dc)_{c\to 0} = 3.79$ K per percent Gd, for the rate of depression.[9] Interpreting this result in terms of the theory of Abrikosov and Gor'kov,[29]

$$\left.\frac{dT_c}{dc}\right|_{c\to 0} = \frac{3\pi^2 N(E_F) J^2 S(S+1)}{4k_B} \quad , \tag{10}$$

a value of $|J| = 0.073$ eV is obtained. Finally, broadening of the linewidth of the La^{139} NMR in a $c = 0.001$ sample[30] yields a value of 27.4 Oe at 4.2 K and 14 kOe. Using the above data and a moment analysis[15] for the linewidth leads to a value of $|J| = 0.1$ eV.

All of these diverse measurements give values of J that are between 0.057 and 0.11 eV when interpreted in the free-electron model. The results of such an analysis in magnetically dense $GdAl_2$ differ from those in $La_{1-c}Gd_cAl_2$ in several respects: First, the g shift is negative indicating a negative value of $J(= -0.04$ eV).[12,31] Second, the temperature-dependent part of the ESR linewidth is a factor of 10 less than that found in the dilute samples,[31] and is presumably the result of "bottlenecking" of the impurity spin-lattice relaxation.[27] Third, the magnitude of J as determined from spin-disorder resistivity measurements[32] and from an analysis of the ordering temperature and Knight-shift[33] data indicate values of $|J| (\simeq 0.4$ eV) that are considerably larger than the values found from the measurements we have discussed in the dilute systems.

In order to properly deal with an analysis of the g shifts or the disparity between values of J in dense and dilute magnetic materials, it is necessary to have a more accurate description of the Fermi-surface conduction electrons. For example, the g shifts depend on the uniform ($q = 0$) component of the s-f exchange, $J(0)$. The sign and magnitude of $J(0)$ are believed to result from two sources[34]: a "Heisenberg exchange" whose contribution to $J(0)$ is positive, and a negative term resulting from interband mixing of $4f$ orbitals with the conduction band. Since these are comparable in magnitude any slight change in the character of the Fermi-surface electrons with increasing Gd concentration could account for the change in sign of $J(0)$ observed. A systematic study of the g shift as a function of concentration is needed to clarify this problem. Unfortunately, at the present time the theory of interband exchange is not developed to the point of predicting such phenomena.[35]

The disparity of values of J in the dense and dilute cases is an analogous problem. This larger J value observed in $GdAl_2$ could be explained by a short-range superexchange process between neighboring Gd atoms. Such an overlap mechanism would presumably not be affected by slight changes in the Fermi-surface electrons. However, the value of the paramagnetic Curie temperature of $GdAl_2$ as determined by susceptibility measurements is found to vary strongly with slight dilutions of Th and La,[33] which indicates that conduction electrons play a major role in determining the changes in $J(0)$. The resolution of this problem appears to lie in the fact that the range function in $LaAl_2$ deviates from the customary form expected from the free-electron approximation. In particular both exchange enhancement[36,37] and the effects of the real scattering potential (rather than the assumed δ-function form) and the non-s character of the Fermi-surface electrons[35] can produce significant enhancement of Gd-Gd interaction at short range. However it is difficult to arrive at a unique prediction for interaction strength from these formalisms.

Finally, we discuss one of the most puzzling aspects of these experimental results: the fact that the $c = 0.05$ and the $c = 0.10$ samples exhibit the same functional dependence of τ_1 on H and T as observed in the more dilute samples. This is in sharp contrast to the bulk magnetization and susceptibility measurements made on other $La_{1-c}Gd_cAl_2$ samples, which appear to indicate the onset of magnetic order.[9,38] Although there are certainly ambiguities associated with such measurements,[39] the results are self-consistent, and when interpreted in terms of a molecular-field model, indicate ordering temperatures of 4–5 K for the $c = 0.05$ sample and 10–14 K for the $c = 0.10$ sample.

If the long-range magnetic order did occur at some temperature, one would expect deviations in the observed $\partial B_{7/2}(x)/\partial x$ behavior of τ_1 and a change in the line profile. No such effects have been observed, and measurements of $1/\tau_1^0$ (Fig. 5) and the exclusion radius (Fig. 7) below the proposed ordering temperatures appear to remain consistent with the paramagnetic interpretation. As mentioned in Sec. II C, τ_1 measurements at various positions in the line profile appear to indicate the same behavior for all nuclei observed. These observations lead us to believe that, for temperatures greater than 1.2 K and at magnetic fields greater than 3.6 kOe, most of the material remains paramagnetic. The relaxation data indicates an absence of long-range magnetic order in these samples in the field and temperature range studied.

We believe that this qualitative difference between the present relaxation studies and the previous magnetic measurements is directly related to the very subtle problem of magnetic order among randomly situated impurities in a metal. A detailed discussion of the theory[40] is not warranted in the present context, but we will examine several experimental aspects which bear on the differences observed. First, these measurements were not performed on the same samples, and there is experimental evidence that sample preparation can significantly affect the magnetic properties in some systems.[41] However, the experience of a number of investigators in the ternary alloy system $La_{1-c}Gd_cAl_2$ indicates that the magnetic properties of samples with the same chemical composition are reproducible. We therefore believe that the samples used in both investigations were magnetically similar.

Second, one might expect different behavior if the two types of measurement were preferentially sampling different parts of the specimen. For example, in systems with $c = 0.05–0.10$, there is a significant probability that a given spin may have one or more magnetic neighbors.[42] The strong exchange between these spins could lead to an enhancement of their contribution to the susceptibility. At the same time the large local fields in the vicinity of such a pair (or larger cluster) would tend to remove nearby nuclei from our range of observation. Although the variation of $1/\tau_1^0$ with concentration does not indicate any dramatic change at low temperatures for the higher concentration samples it does not preclude such cluster effects. Similarly, the interpretation of the susceptibility data is involved in itself[42,43] and it would be difficult to argue against such a clustering on the basis of that data.

Finally, the magnetic measurements were made primarily at low fields (~ 250–500 Oe), while the minimum value of magnetic field used in the relaxation measurement was 3.6 kOe. Dramatic changes in the magnetic susceptibility have been observed in $La_{0.94}Gd_{0.06}$ when a magnetic field of ~ 250 Oe was applied to the sample.[44] Although an explanation has been proposed for this behavior[43] the experimental situation is still unclear. This possible field effect could be studied by performing magnetization measurements at higher fields, and also by performing relaxation studies at zero magnetic field using NQR.[45] The resolution of this problem awaits these experimental results.

V. CONCLUSION

Although the interpretation of nuclear spin-lattice relaxation results is often quite difficult, a number of favorable factors, most notably the absence of spin diffusion, enable us to perform a direct analysis in the present case. The functional dependence of the relaxation rate with varying H and T establishes that the LD process is the dominant mechanism, and the linear dependence of $1/\tau_m$ on c suggests that Gd-Gd coupling via the RKKY interaction is responsible for the decay of spin correlations. The resulting value for the strength of the host-impurity coupling is in good agreement with previous investigations. Similar observations are currently being made on $LaAl_2$ samples doped with non–S-state impurities such as Ce and Tm. These results will be published elsewhere.

ACKNOWLEDGMENTS

We would like to express our special gratitude to P. Pincus for his continuous encouragement and assistance. Discussions with D. MacLaughlin and B. Maple concerning their experiments in the same systems have been most enlightening. We would also like to acknowledge stimulating discussions on the topics contained in this paper with D. Davidov, B. Giovannini, A. J. Heeger, D.W. Hone, V. Jaccarino, H. Launois, T. Moriya, R. Orbach, and D. Shaltiel.

APPENDIX A

In this appendix we justify the form chosen above for the impurity component of the magnetization recovery. In the absence of nuclear-spin diffusion, Eq. (4) predicts that recovery of a nucleus at site i owing to the presence of an ensemble of magnetic impurities is

$$p(\vec{r}_i, t) = \exp\{-t\textstyle\sum_j [1/T(r_{ij})]\} \, , \qquad \text{(A1)}$$

where $r_{ij} = |\vec{r}_i - \vec{r}_j|$ and the j sum extends over the impurity sites. To describe the magnetization recovery of the entire system, we must perform an ensemble average over all possible impurity configurations about a nuclear site.

We consider a lattice containing N_0 rare-earth sites, a fraction c of which are occupied at random by magnetic impurities. If a particular site, k, is occupied (with probability c) the contribution to the recovery will be $e^{-t/T_1(r_{ik})}$, while if the site is unoccupied [with probability $(1-c)$], the appropriate expression for the relaxation function is unity. Taking a weighted average of these contributions, we obtain the following expression:

$$p(t) = \textstyle\prod_j [(1-c) + c\, e^{-t/T_1(r_{ij})}] \quad , \quad r_{ij} > r_0 \qquad \text{(A2)}$$

for the relaxation function. We have excluded from consideration any nuclei lying sufficiently close to the magnetic impurity ($r_{ij} < r_0$) to have their field for resonance shifted from our range of observation.

If $c = 1.0$, we find $p(t) = \exp[-t\sum_j 1/T_1(r_{ij})]$, i.e., the magnetization recovery is exponential and the contribution must be summed over all sites. For low concentration, Eq. (A2) may be written in the following form:

$$p(t) \simeq \exp[-c\textstyle\sum_j (1 - e^{-t/T_1(r_{ij})})] \, , \quad r_{ij} > r_0 \qquad \text{(A3)}$$

which is equivalent to Eq. (A2) to order c. If we choose to express the lattice sums Eq. (A3) in a continuum approximation we obtain

$$p(t) \simeq \exp[-N_0 c \textstyle\int (1 - e^{-t/T_1(r,\theta)}) d^3 r] , \quad r > r_0 \qquad \text{(A4)}$$

where $1/T_1(r, \theta)$ implies that angular dependence may be explicitly included (see Table II).

Eq. (A4) makes it possible to obtain analytic expressions for the recovery of the magnetization and these prove to be extremely useful in a qualitative analysis of the problem. For example, if we choose $1/T_1(r) = \mathcal{C}/r^6$ (no angular dependence) Eq. (A4) can be integrated to obtain[46]

$$p(t) = \exp\{-\tfrac{4}{3}\pi r_0^3 N_0 c [e^{-\mathcal{C}t/r_0^6} - 1 + (\pi \mathcal{C} t/r_0^6)^{1/2} \operatorname{erf}(\mathcal{C}t/r_0^6)^{1/2}]\} \, . \qquad \text{(A5)}$$

In the limit $\mathcal{C}t/r_0^6 \gg 1$, $p(t)$ assumes the simple form $p(t) \propto \exp[-(t/\tau_1)^{1/2}]$, with $(1/\tau_1)^{1/2} = \frac{4}{3}\pi^{3/2} \times N_0 c\, \mathcal{C}^{1/2}$, while for $\mathcal{C}t/r_0^6 \ll 1$ one obtains

$$p(t) = e^{-t/T_1} \text{ with } 1/T_1 = 4\pi N_0 c\, \mathcal{C}/3r_0^3 \, .$$

It is important to note that, in spite of assuming $c \ll 1$ and adopting a continuum description, the analytic form of $p(t)$ [Eq. (A5)] gives almost exactly the same result as obtained using numerical results for $c \lesssim 0.10$ evaluation of Eq. (A2). We compare the prediction of the analytic form with the computer-calculated product Eq. (A2) over 4093 lattice sites for several values of r_0 in Fig. 8, and the agreement is very good.

A similar analytic expression can be obtained for the GH mechanism, where $1/T_1(r) \propto \mathcal{C}_{GH}/r^5$. The resulting analytic form is obtained in terms of incomplete γ functions, but in the limit $\mathcal{C}_{GH}t/r^5 \gg 1$, it has the form $p(t) \propto \exp[-(t/\tau)^{3/5}]$.

APPENDIX B

We use the averaging procedure of Appendix A to arrive at an expression for the decay of the autocorrelation function of the impurity spin caused by the RKKY interaction. We consider a system containing N_0 rare-earth sites, a fraction c of which are occupied by Gd impurities. We assume that the Gd spin-spin coupling arises from the RKKY interaction

$$\mathcal{H}_{\text{RKKY}} = \sum_{i \neq j} J(r_{ij})\, \vec{S}_i \cdot \vec{S}_j \, , \qquad \text{(B1)}$$

where

$$J(r_{ij}) = 4\pi E_F N^2(E_F)\, J^2 \left(\frac{\sin 2k_F r_{ij} - 2k_F r_{ij} \cos 2k_F r_{ij}}{(2k_F r_{ij})^4} \right). \tag{B2}$$

The short-time expansion of the autocorrelation function is then[47]

$$\langle S_j^z(t) S_j^z(0) \rangle = \langle S_j^z S_j^z \rangle - (1/2\hbar^2)\, \alpha\, t^2 + \cdots , \tag{B3}$$

where $\alpha = \langle [\mathcal{H}, S_j^z][S_j^z, \mathcal{H}] \rangle$ and the brackets indicate a thermal average: $\langle 0 \rangle = \mathrm{Tr}(e^{-\beta\mathcal{H}}0)/\mathrm{Tr}(e^{-\beta\mathcal{H}})$. In the high-temperature approximation for $2k_F r \gg 1$, we find

$$3\langle S_j^z(t) S_j^z(0) \rangle / S(S+1) = 1 - t^2 \sum_{i \neq j} (\omega_e)_{ij}^2 , \tag{B4}$$

where

$$(\omega_e)_{ij}^2 = \frac{S(S+1)}{3\hbar^2} \left(\frac{4\pi E_F N^2(E_F) J^2}{(2k_F)^3} \right)^2 \frac{\cos^2 2k_F r_{ij}}{r_{ij}^6} \tag{B5}$$

($\sin 2k_F r_{ij}$ can be ignored as long as $2k_F r_{ij} \gg 1$).

As discussed in Sec. III C, we assume a Gaussian form for the correlation function of any given spin:

$$3\langle S_j^z(t) S_j^z(0) \rangle / S(S+1) = e^{-(t/\tau_{\mathrm{ex}})^2} , \tag{B6}$$

where

$$1/\tau_{\mathrm{ex}} = \Big[\sum_{i \neq j} (\omega_e)_{ij}^2 \Big]^{1/2} . \tag{B7}$$

As in Appendix A, we take a weighted sum over all sites

$$\psi(t) = \langle\langle \langle S_j^z(t)\, S_j^z(0) \rangle \rangle\rangle = \prod_i \big[(1-c) + c\, e^{-t^2 (\omega_e)_{ij}^2} \big] . \tag{B8}$$

We can calculate this product numerically, and the results are shown in Fig. 9. We can also proceed as in Eqs. (A3) and (A4) to express this in terms of a $c \ll 1$ continuum approximation. If we take an average $\cos^2 2k_F r \simeq \frac{1}{2}$, the integral equivalent to Eq. (A4) can be performed, with the result that $\psi(t) = e^{-t/\tau_m}$, where

$$1/\tau_m = \tfrac{2}{3}\, \pi^2 \big[\tfrac{1}{6} \pi S(S+1) \big]^{1/2} \big[N^2(E_F) J^2 E_F N_0 c / \hbar k_F^3 \big] . \tag{B9}$$

By analogy with the nuclear relaxation problem of Appendix A, we expect a change in *form* of the decay of the autocorrelation function as the concentration of impurities decreases. For $c = 1.0$ we have chosen the decay to be Gaussian, while for $c \ll 1$ an exponential decay is obtained as has been noted previously.[23] For our purposes it is crucial to know if $\psi(t)$ changes significantly over the range of concentrations studied here. We have investigated this problem by using a computer to evaluate $\psi(t)$ directly from Eq. (B8) and then evaluating the quantity $\langle \tau_e \rangle$ [$\langle \tau_e \rangle = \int_0^\infty \psi(t)\,dt$] numerically for arbitrary values of c. As indicated in Ref. 23, a Gaussian decay of $\psi(t)$ implies that $\langle \tau_e \rangle \propto c^{-1/2}$ while an exponential decay implies that $\langle \tau_e \rangle \propto c^{-1}$. The variation of $\langle \tau_e \rangle$ for changing c obtained in this way is shown in Fig. 10, and we conclude that $\psi(t)$ is approximately exponential for $c \lesssim 0.1$, is Gaussian for $c \gtrsim 0.8$, and assumes an intermediate form in the range $0.1 \lesssim c \lesssim 0.8$. This provides justification for our choice of the exponential form for $\psi(t)$.

---

[*] Based upon work performed by M. R. McHenry at University of California, Santa Barbara, in partial fulfillment of the requirements for the degree of Doctor of Philosophy.

[†] Present address: Department of Physics, University of California, Riverside, Calif. 92502.

[‡] Work at University of California, Santa Barbara supported in part by the NSF and the University of California, Santa Barbara Committee on Research, Grant No. 5028.

[1] M. R. McHenry, B. G. Silbernagel, and J. H. Wernick, Phys. Rev. Letters 27, 426 (1971). For other previous impurity studies, see, e.g., O. J. Lumpkin, Phys. Rev. 164, 324 (1967); R. E. Levine, Phys. Letters 28A, 504 (1969); P. Bernier, H. Launois, and H. Alloul, J. Phys. (Paris) 32, C1-513 (1971); F. Y. Fradin, Phys. Rev. Letters 26, 1033 (1971).

[2] For a review of impurity relaxation in insulators see I. J. Lowe and D. Tse, Phys. Rev. 166, 279 (1968).

[3] J. Korringa, Physica 16, 601 (1950).

[4] See, e.g., P. G. de Gennes, J. Phys. Chem. Solids 3, 345 (1958), and Ref. 2.

[5] Possible impurity relaxation processes in metals have recently been reviewed by B. Giovannini, P. Pincus, G. Gladstone, and A. J. Heeger, J. Phys. (Paris) 32, C1-163 (1971).

[6] K. Yosida, Phys. Rev. 106, 893 (1957).

[7] C. Kittel, in *Solid State Physics*, Vol. 22, edited by H. Ehrenreich, F. Seitz, and D. Turnbull (Academic, New York, 1968).

[8] D. Tse and S. R. Hartmann, Phys. Rev. Letters 21, 511 (1968).

[9] M. B. Maple, Phys. Letters 26A, 513 (1968).

[10] J. H. Wernick and S. Geller, Trans. AIME 218, 866 (1960).

[11] W. G. Clark, Rev. Sci. Instr. 35, 316 (1964).

[12] V. Jaccarino, B. T. Matthias, M. Peter, H. Suhl, and J. H. Wernick, Phys. Rev. Letters 5, 251 (1960).

[13] W. W. Simmons, W. J. O'Sullivan, and W. A. Robinson, Phys. Rev. 127, 1168 (1962). For a demonstration of the variation of the α_i with different saturating conditions, see A. Narath, *ibid.* 162, 320 (1967).

[14] Such a procedure is justified only if the impurity and host relaxation processes are independent. As we will discuss below, this is justified in the present case since the source of the hyperfine field at the nucleus is different for the two processes. The substitution of Gd for La is not believed to modify $1/T_{1K}$ appreciably, see, e.g., B. G. Silbernagel, V. Jaccarino, P. Pincus, and J. H. Wernick, Phys. Rev. Letters 20, 1091 (1968).

[15] R. E. Behringer, J. Phys. Chem. Solids 2, 209 (1957).

[16] N. Bloembergen, E. M. Purcell, and R. V. Pound, Phys. Rev. 73, 679 (1948).

[17] N. Bloembergen, Physica 25, 386 (1949).

[18] W. E. Blumberg, Phys. Rev. 119, 79 (1960).

[19] H. Benoit, P. G. de Gennes, and D. Silhouette, Compt. Rend. 256, 3841 (1963).

[20] B. Giovannini and A. J. Heeger, Solid State Commun. 7, 287 (1969).

[21] B. R. Coles, D. Griffiths, R. J. Lowin, and R. H. Taylor, J. Phys. C 3, L121 (1970).

[22] J. E. Gulley, D. Hone, D. J. Scalapino, and B. G. Silbernagel, Phys. Rev. B 1, 1020 (1970).

[23] C. Kittel and E. Abrahams, Phys. Rev. 90, 238 (1953).

[24] P. W. Anderson and P. R. Weiss, Rev. Mod. Phys. 25, 269 (1953).

[25] A. G. Redfield and W. N. Yu, Phys. Rev. 169, 433 (1968).

[26] N. Bloembergen and T. J. Rowland, Phys. Rev. 97, 1679 (1955).

[27] H. Hasegawa, Progr. Theoret. Phys. (Kyoto) 21, 483 (1959).

[28] P. W. Anderson, J. Phys. Soc. Japan 9, 316 (1954).

[29] A. A. Abrikosov and L. P. Gor'kov, Zh. Eksperim. i Teor. Fiz. 39, 1781 (1960) [Sov. Phys. JETP 12, 1243 (1961)].

[30] A. C. Gossard, V. Jaccarino, and J. H. Wernick, J. Phys. Soc. Japan Suppl. B-1, 88 (1962).

[31] D. Davidov and D. Shaltiel, Phys. Rev. 169, 329 (1968).

[32] J. A. Mydosh, M. P. Kawatra, and J. I. Budnick, Phys. Letters 24A, 421 (1967).

[33] K. H. J. Buschow, J. F. Fast, A. M. Van Diepen, and H. W. de Wijn, Phys. Status Solidi 24, 715 (1967).

[34] R. E. Watson, S. Koide, M. Peter, and A. J. Freeman, Phys. Rev. 139, A167 (1965).

[35] R. E. Watson and A. J. Freeman, Phys. Rev. 152, 566 (1966); 178, 725 (1969).

[36] B. Giovannini, M. Peter, and J. R. Schrieffer, Phys. Rev. Letters 12, 936 (1964).

[37] A. J. Heeger, in Ref. 7, Vol. 23.

[38] M. B. Maple, thesis (University of California, San Diego, 1969) (unpublished).

[39] A. Arrott, Phys. Rev. 108, 1394 (1957).

[40] See, e.g., W. Marshall, Phys. Rev. 118, 1519 (1960); M. W. Klein and R. Brout, *ibid.* 132, 2412 (1963); S. H. Liu, *ibid.* 157, 411 (1967).

[41] D. Korn, Z. Physik 187, 463 (1965).

[42] The analogous problem in dilute magnetic insulators has been explored by H. Sato, A. Arrott, and K. Kikuchi, J. Phys. Chem. Solids 10, 19 (1959).

[43] K. H. Benneman, J. W. Garland, and F. M. Mueller, Phys. Rev. Letters 23, 1503 (1969).

[44] D. K. Finnemore, L. J. Williams, F. H. Spedding, and D. C. Hopkins, Phys. Rev. 176, 712 (1967).

[45] D. E. Mac Laughlin and M. Daugherty, Phys. Rev. (to be published).

[46] By changing variables, $y = 1/r^3$, and integrating by parts. See also Ref. 8.

[47] See, e.g., T. Moriya, Progr. Theoret. Phys. (Kyoto) 16, 23 (1956).